A classical dynamics method for H-2 diffraction from metal surfaces

Diaz, C.; Busnengo, H.F.; Riviere, P.; Farias, D.; Nieto, P.; Somers, M.F.; ... ; Martin, F.

A classical dynamics method for H_2 diffraction from metal surfaces

Cite as: J. Chem. Phys. **122**, 154706 (2005); https://doi.org/10.1063/1.1878613
Submitted: 14 July 2004 . Accepted: 01 February 2005 . Published Online: 18 April 2005

C. Díaz, H. F. Busnengo, P. Rivière, D. Farías, P. Nieto, M. F. Somers, G. J. Kroes, A. Salin, and F. Martín

A classical dynamics method for H_2 diffraction from metal surfaces

C. Díaz
Departamento de Química, Facultad de Ciencias C-9, Universidad Autónoma de Madrid, 28049 Madrid, Spain and Laboratoire de Physico-Chimie Moléculaire, UMR 5803 CNRS-Université Bordeaux I, 33405 Talence Cedex, France

H. F. Busnengo
Instituto de Física Rosario, CONICET and Facultad de Ciencias Exactas, Ingeniería y Agrimensura, Universidad Nacional de Rosario, Avenida Pellegrini 250, 2000 Rosario, Argentina

P. Rivière
Departamento de Química, Facultad de Ciencias C-9, Universidad Autónoma de Madrid, 28049 Madrid, Spain

D. Farías and P. Nieto
Departamento de Física de la Materia Condensada C-3 and Instituto Nicolas Cabrera, Universidad Autónoma de Madrid, 28049 Madrid, Spain

M. F. Somers and G. J. Kroes
Leiden Institute of Chemistry, Gorlaeus Laboratories, Leiden University, P.O. Box 9502, 2300 RA Leiden, The Netherlands

A. Salin
Laboratoire de Physico-Chimie Moléculaire, UMR 5803 CNRS-Université Bordeaux I, 33405 Talence Cedex, France

F. Martín
Departamento de Química, Facultad de Ciencias C-9, Universidad Autónoma de Madrid, 28049 Madrid, Spain

(Received 14 July 2004; accepted 1 February 2005; published online 18 April 2005)

We present a discretization method that allows one to interpret measurements on diffraction of diatomic molecules from solid surfaces using six-dimensional (6D) classical trajectory calculations. It has been applied to the D_2/NiAl(110) and H_2/Pd(111) systems (which are models for activated and nonactivated dissociative chemisorption, respectively) using realistic potential energy surfaces obtained from first principles. Comparisons with experimental results and 6D quantum dynamical calculations show that, in general, the method is able to predict the relative intensity of the most important diffraction peaks. We therefore conclude that classical mechanics can be an efficient guide for experimentalists in the search for the most significant diffraction channels. © *2005 American Institute of Physics*. [DOI: 10.1063/1.1878613]

I. INTRODUCTION

The study of the interaction of H_2 with metal surfaces is relevant in many fields of physics and chemistry.[1–8] Most of these studies have focused on the dissociative chemisorption process. The traditional approach is either to perform "sticking" experiments in which incidence angle, impact energy, surface temperature, etc., are varied,[9–11] or to perform associative desorption experiments on the reverse reaction with application of detailed balance to learn about the effect of initial molecular rotation[12] and rotational alignment[13] on the reaction. In a more recent development, scanning tunneling microscopy has also been applied to determine the most reactive sites (see, e.g., Refs. 14 and 15 and references therein).

The scattering of H_2 from metal surfaces has also been considered. Scattering experiments have provided final state resolved information on vibrational excitation of H_2 on Cu(111) (Refs. 16 and 17) and state-to-state information concerning rotationally elastic,[18] rotationally inelastic,[19,20] and rotationally and vibrationally inelastic[21–23] scattering from metal surfaces. Theoretical calculations have shown that, for reactive metal systems, the extent to which vibrationally inelastic scattering occurs can provide qualitative information on the shape of the reaction path.[24] Similarly, rotationally inelastic scattering can provide information about the anisotropy of the potential energy surface.[25]

A different point of view is provided by diffraction experiments, in which the angular distributions of reflected molecules are analyzed for quantized changes in translational momentum parallel to the surface. The analysis of the angular distribution can be used to obtain detailed information on the molecule/surface dynamics and, therefore, on the corresponding potential energy surface (PES).[26] A few experimental attempts along this line have been already published. For instance, elastic and rotationally inelastic diffractions have been studied for H_2 molecules incident on Cu(001),[27] Ag(111),[28] NiAl(110),[29] Rh(110),[30] Ni(110),[8] and Pd(111) (Ref. 31) surfaces. For the latter three systems dissociative

adsorption is *nonactivated* and, therefore, reflection probabilities are very small.[32]

Classical dynamics simulations are expected to give a reasonable description of the H_2-surface interactions for not too low incident energy. This was already realized in the early 1970s through the works of Doll and co-workers (see, e.g., Refs. 33–36 and references therein), who showed that adsorption, desorption, and nondiffractive scattering of H_2, HD, and D_2 can be reasonably described by using classical methods. In classical mechanics, the effect of quantization is usually introduced by replacing the continuous distribution by a histogram in which all values contained in a given interval are associated with a single-quantum value. Such a procedure has been successfully used in different contexts, in particular, in the description of rotational and vibrational excitations of diatomic molecules interacting with various surfaces (see, e.g., Refs. 37 and 38). Comparisons with quantum calculations obtained with the same PES have shown that classical mechanics is able to provide accurate results for, e.g., total and angle-resolved dissociation probabilities as well as rotational excitation probabilities in the energy range typical of diffraction experiments, i.e., 50–200 meV.[3,37,39–41] The above methods resemble the "binning" procedures used to determine quantum product state distributions from classical trajectory simulations in gas-phase reactive scattering (see, e.g., an early review by Truhlar and Muckerman[42]). Recently, Gaussian weighting has been incorporated into the binning (see Ref. 43 and references therein), but this refinement has not yet been considered in H_2-surface scattering problems.

In the case of diffraction, the wave aspect of atomic particles is so omnipresent that it is usually assumed that no physical insight can be obtained within a "classical world." Perhaps this is because atomic and molecular diffractions were used in the 1920s to prove the wave nature of atomic and molecular motions. According to Bragg's law and applying the de Broglie relation between wavelength and momentum, diffraction is observed when the variation of the linear momentum parallel to the surface is restricted to well defined discrete values. In contrast, linear momentum changes continuously in a classical world. Discretization methods that make classical trajectory calculations compatible with Bragg's law were first proposed by Ray and Bowman in 1975 to study diffraction of He (Ref. 44) and H_2 (Ref. 45) by a "model" LiF(001) surface. A comparison with quantum and semiclassical results showed that the method was useful to estimate diffraction peak intensities. Similar methods were used later by Park and Bowman[46] and Saini *et al.*,[47] then quoted by Gerber in 1987 (Ref. 48), and finally forgotten. No direct comparison with experiment was ever reported in these works, which was due to the absence of reliable molecule-surface potentials in those days. In view of the above, it may well come as a surprise to many that classical mechanics can be used to predict intensities for molecular diffraction, which has always been viewed as a typical quantum phenomenon.

The goal of this paper is to check if a discretization procedure similar to that proposed earlier[44,45] can be used to derive realistic diffraction intensities for H_2 scattering from (reactive) metal and alloy surfaces, with the interaction described by accurate *ab initio* PESs. Our interest in using classical instead of quantum mechanics is the usual one: classical simulations are computationally cheap and it is often easier to interpret and visualize the dynamics by following the trajectories than following the evolution of a wave packet. In cases where quantum dynamical calculations are expensive, the use of classical mechanics may allow one to explore many more experimental conditions, which can be important to guide experimentalists and to obtain physical interpretations in parallel with experiments. This is relevant in the context of diffraction experiments, where both energy and incidence angle are varied independently. Earlier quantum calculations have mainly focused on normal incidence. However, to be predictive for diffraction experiments, quantum calculations must be performed for off-normal incidence. The latter calculations are still too expensive to be systematically used in explorative research. In this work we have performed a few such calculations to validate the classical approach.

Application of the discretization method to our classical trajectory calculations will be most helpful in the search for significant diffraction channels. This is especially important in the case of out-of-plane diffraction since, in this way, one can potentially avoid scanning large fractions of the total accessible solid angle 2π. To illustrate our procedure we have chosen two systems: the reactive system $H_2/Pd(111)$, for which reaction dominates over diffractive scattering and for which out-of-plane diffraction was recently seen to be much more important than in-plane diffraction at grazing incidence,[31] and the nonreactive system $D_2/NiAl(110)$, for which there is significant diffraction, but out-of-plane diffraction does not dominate.[29] For both systems, there exist previous experimental measurements[29,31] and realistic *ab initio* PES (Refs. 49 and 50) which will be used here to check the validity of our discretization procedure. In both cases, the PES was based on calculations using density functional theory (DFT), employing the generalized gradient approximation (GGA).[51,52] In the case of $H_2/Pd(111)$, a further rigorous test will be provided by a direct comparison with results of a quantum dynamical calculation using the same PES.

The paper is organized as follows. In the following section, we briefly outline the theoretical methods used in this work. In Sec. III, we explain in detail the method to obtain diffraction peak intensities from classical dynamics calculations. In Sec. IV, classical diffraction probabilities are compared to quantum results for the $H_2/Pd(111)$ system. Applications of the classical method to the $D_2/NiAl(110)$ and $H_2/Pd(111)$ systems are presented and compared with experiments in Sec. V. We end the paper with some conclusions in Sec. VI.

II. THEORETICAL METHODS

The methods used in this work have been described in detail earlier.[37,53] Briefly, we use the PESs of Refs. 49 and 50 for $H_2/Pd(111)$ and $H_2/NiAl(110)$, respectively, determined

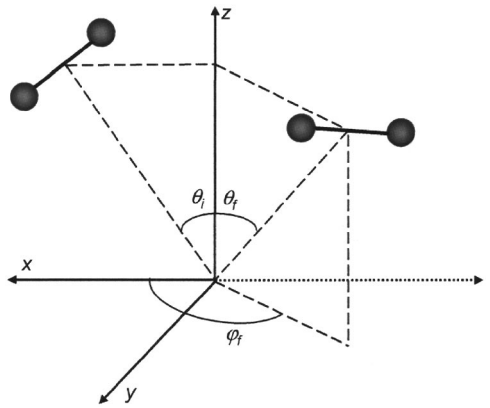

FIG. 1. Definition of coordinate system. The *XY* plane is the surface plane and the *XZ* plane coincides with the plane of incidence. Thus, in-plane reflection corresponds to $\varphi_f=0$, π (it is called *specular* if $\varphi_f=0$ and $\theta_i=\theta_f$) and out-of-plane reflection to $\varphi_f\neq 0$.

by interpolation of *ab initio* DFT/GGA data using the corrugation reducing procedure (CRP).[54] The CRP has been shown to provide a precision better than 30 meV in the dynamically relevant regions for several H_2-metal systems.[49,50,55] Calculations on dissociative chemisorption of H_2 on metal surfaces, at normal and off-normal incidence, suggest that, in principle, very accurate dynamics results can be obtained on the basis of accurately fitted DFT/GGA potentials [e.g., in $H_2+Pt(111)$ (Ref. 56)], although there remains considerable uncertainty connected to which GGA is best used [e.g., in $H_2+Ru(0001)$ (Ref. 57)]. Also recent calculations on diffraction of H_2 scattering from metal and metal alloy surfaces[58] likewise suggest that accurate results can be obtained for diffraction based on accurately fitted DFT/GGA potentials.

We have used the above PESs to perform six-dimensional (6D) classical trajectory and quantum calculations in which only the diatom degrees of freedom and not the vibrations of the surface are included. In classical calculations, the initial vibrational zero point energy (ZPE) of H_2 or D_2 is not included. We have shown in Ref. 37 that exclusion of the ZPE leads to smaller dissociation probabilities but it barely affects (i) the angular distribution of reflected molecules and (ii) the variation of the dissociation probability with incidence angle. Thus, although diffraction probabilities might be slightly overestimated in the classical calculations, this is not a major problem because experiment usually provides the *relative* intensities of the different diffraction peaks. For $H_2/Pd(111)$, we have performed additional quantum dynamics calculations using a time dependent wave packet method.[56] The method uses a discrete variable/finite basis representation for all degrees of freedom. The initial wave packet is propagated in time using the split-operator method. The reflected wave packet is analyzed using a scattering amplitude formalism.

We have considered H_2 and D_2 molecules incident upon the Pd(111) and NiAl(110) surfaces with initial translation energy E_i and incidence angle θ_i (see Fig. 1). The direction of reflected molecules is defined by θ_f, φ_f. The angles $\theta_{i,f}$ take values between 0 and $\pi/2$ and are measured with respect to the surface normal, so that specular reflection corresponds to $\theta_i=\theta_f$. The azimuthal angle φ_f is defined with respect to the projection on the surface of the incident velocity vector. We have considered the incidence directions $[101]$ and $[11\bar{2}]$ for $H_2/Pd(111)$ and $[1\bar{1}0]$ for $D_2/NiAl(110)$. To take into account the rotational excitation of the H_2 and D_2 beams used in the experiments,[29,31] we have performed dynamical calculations for initial angular momenta $J_i=0-3$ in the case of $H_2/Pd(111)$ and $J_i=0-4$ in the case of $D_2/NiAl(110)$. Quantum calculations have been restricted to the dominant $J_i=0,1$ initial states. The initial population of the different rotational states have been taken from experiment.[29,31]

III. CLASSICAL DIFFRACTION METHOD

We consider a beam of H_2 or D_2 molecules with total mass $2M$ and initial translational energy E_i, M being the mass of one of the atoms. The modulus of the associated wave vector is given by

$$k_i=\frac{\sqrt{4ME_i}}{\hbar}. \tag{1}$$

We write the initial and final wave vectors $\mathbf{k}_i$ and $\mathbf{k}_f$ in terms of components parallel and perpendicular to the surface: $\mathbf{k}_i=(\mathbf{K}_i^{\parallel},k_{i,z})$ and $\mathbf{k}_f=(\mathbf{K}_f^{\parallel},k_{f,z})$. For a perfect rigid periodic surface with lattice vectors $\mathbf{a}_1$ and $\mathbf{a}_2$, the Bragg condition for diffraction is[26]

$$\mathbf{K}_i^{\parallel}+\mathbf{G}_{nm}=\mathbf{K}_f^{\parallel}, \tag{2}$$

where $\mathbf{G}_{nm}$ is a vector of the reciprocal lattice and (n,m) are the associated Miller indices. The vector $\mathbf{G}_{nm}$ is given by $\mathbf{G}_{nm}=n\mathbf{b}_1+m\mathbf{b}_2$, where $\mathbf{b}_1$ and $\mathbf{b}_2$ are the basis vectors of the reciprocal lattice that satisfy $\mathbf{a}_i\cdot\mathbf{b}_j=2\pi\delta_{ij}$. At the impact energies considered in this work, vibrational excitation is not possible and, therefore, variation of the internal energy of the molecule is only possible through rotational excitations. Thus, combining Bragg's law with total energy conservation leads to

$$k_{z,f}^2=k_i^2-\frac{4M\Delta E_{\mathrm{rot}}}{\hbar^2}-(\mathbf{K}_i^{\parallel}+\mathbf{G}_{nm})^2>0, \tag{3}$$

where

$$\Delta E_{\mathrm{rot}}=E_{\mathrm{rot}}^f-E_{\mathrm{rot}}^i=\frac{\hbar^2(k_i^2-k_f^2)}{4M}, \tag{4}$$

with E_{rot}^f and E_{rot}^i being the rotational energy of the scattered and incident molecules, respectively.

Now, we have to look for a procedure that is compatible with Bragg's law, i.e., which leads to a k histogram that allows one to assign a classical trajectory with final momentum $\mathbf{p}_f$ to one of the diffraction peaks given by Eq. (2). To better illustrate this procedure, which basically follows the prescriptions of Ref. 45, let us consider the reciprocal lattices of the Pd(111) and NiAl(110) surfaces shown in Fig. 2 (extension to other surfaces is straightforward). From Bragg's law, the variation of parallel momentum, $\hbar\Delta\mathbf{K}^{\parallel}=\hbar(\mathbf{K}_f^{\parallel}-\mathbf{K}_i^{\parallel})$, must coincide with one of the vectors of the reciprocal lattice (up to $\hbar$). Since there is not such a restriction in classical

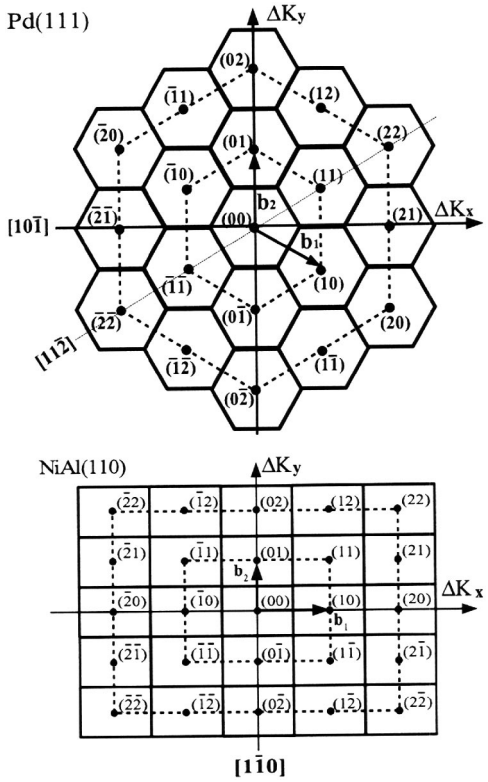

FIG. 2. Reciprocal space for the Pd(111) and NiAl(110) surfaces showing 2D Wigner–Seitz cells around each lattice point. Numbers within parentheses indicate the corresponding Miller indices. Dashed lines show diffraction orders. Numbers within brackets indicate the incidence directions considered in this work.

calculations, $\Delta\mathbf{P}^{\parallel}$ can be any vector in the plane that defines the surface in reciprocal space (i.e., any vector in Fig. 2). We divide this plane in identical regions, such that each region corresponds to the Wigner–Seitz cell around each lattice point in reciprocal space. Thus, each cell is unambiguously associated with a lattice vector and, therefore, with a diffraction peak (see Fig. 2). Then, we can easily assign all classical trajectories with a value of $\Delta\mathbf{P}^{\parallel}$ contained in a given Wigner–Seitz cell to the corresponding (n,m) vector of the reciprocal lattice. The diffraction probability $P_{n,m}$ is given by the number of trajectories $N_{n,m}$ in which the molecule scatters nonreactively with $\Delta\mathbf{P}^{\parallel}$ in the (n,m) Wigner–Seitz cell divided by the total number of trajectories N_{tot}:

$$P_{n,m} = N_{n,m}/N_{\mathrm{tot}}. \tag{5}$$

In this work, the calculated probabilities will be assumed to be proportional to the diffraction intensities observed experimentally.

In the following, we will not only speak about individual diffraction probabilities but also about diffraction orders (both in classical and quantum calculations). To define different diffraction orders, we build a series of concentric polygons around the (00) point. For the Pd(111) surface, these polygons are hexagons, and for the NiAl(110) surface, they are rectangles (see Fig. 2). We will say that diffraction peaks are of the same order when they belong to the same polygon. For example, in the Pd(111) case, the peaks associated with the lattice vectors (01), ($\bar{1}$0), ($\bar{1}\bar{1}$), (0$\bar{1}$), (10), and (11) are first-order diffraction peaks.

Finally, following a conventional approach (see, e.g., Refs. 37 and 38), we can assign a rotational quantum number J_f to diffracted molecules by evaluating the closest integer that satisfies the well-known formula of a quantum rigid rotor: $J_f=[-1+(1+4J^2/\hbar^2)^{1/2}]/2$, where J is the classical angular momentum of the molecule. This is equivalent to replacing the classical angular momentum by a histogram associated with the quantum values. In contrast with quantum dynamics calculations for which only $\Delta J_f=\pm 2$ transitions are allowed, there are no selection rules in classical dynamics. Therefore, in counting the trajectories associated with a given rotational transition, one must assign those trajectories associated with a forbidden J_f value to the closest allowed one.

The recipe used to discretize the classical angular momentum might be less accurate than that used to discretize the variations in parallel momentum due to the larger energy spacing involved in rotational transitions. This possible limitation should be kept in mind when the intensities of calculated rotationally inelastic diffraction peaks are compared with the experimental results. It must be also taken into account when rotationally mediated selective adsorption[59] (RMSA) comes into play. The latter is related to the anisotropy of the van der Waals attraction and, therefore, to energy exchange from translation to rotation. Consequently RMSA will only be important when rotational excitation is important. As suggested by the experimental results shown below, this is not the case for the systems and incidence energies considered in this work.

IV. COMPARISON WITH QUANTUM DYNAMICS RESULTS

To check the validity of the present method, one must compare with results obtained from quantum dynamical calculations using the same PES. Our benchmark is the H_2/Pd(111) system for normal incidence, $E_i=200$ meV and $J_i=0$. This is the simplest case because, for normal incidence, all directions associated with first-order diffraction peaks are equivalent (or nearly equivalent for higher diffraction orders, see Fig. 2) and, therefore, the corresponding peaks have the same intensity. The results are shown in Fig. 3. It can be seen that classical results are close to the quantum ones for all diffraction orders. In particular, they predict that first-order diffraction is the most important reflection channel followed by second-order diffraction and specular reflection. Classical intensities are slightly higher than the quantum ones because, as shown in previous works,[37,40] classical calculations overestimate the total reflectivity due to the neglect of the ZPE. In the following section, we compare results of this method with diffraction experiments for off-normal incidence.

V. COMPARISON WITH EXPERIMENTAL RESULTS

The experimental results chosen for comparison with our classical and quantum calculations have been published

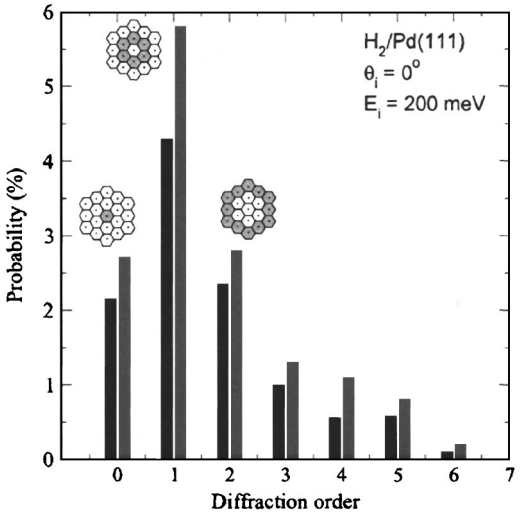

FIG. 3. Probabilities of diffraction orders for $H_2/Pd(111)$ under normal incidence conditions. Black columns: results of quantum calculations. Green columns: results of the classical diffraction method. The relevant Wigner–Seitz cells associated with zeroth-, first-, and second-order diffraction peaks are shown for the sake of clarity.

elsewhere.[29,31,58] The experiments were performed with the apparatus described in detail in Ref. 60 which has been recently transferred to the Surface Science Lab at the Universidad Autónoma de Madrid from the Free University of Berlin. The experimental setup allows rotations of 200° in the scattering plane (defined by the beam direction and the normal to the surface) as well as ±15° from the scattering plane for a fixed angle of incidence. Measurements on NiAl(110) were performed with the crystal at 90 K, while measurements on Pd(111) were performed at 430 K to prevent the buildup of an adsorbed layer of hydrogen.

Figures 4 and 5 show a comparison between "classical" and experimental diffraction spectra for the $D_2/NiAl(110)$ and $H_2/Pd(111)$ systems. For a meaningful comparison with theory, the experimental background has been substracted in all cases. This background is due to two factors not included in the present theoretical calculations: phonon inelastic scattering and desorbed hydrogen in the UHV chamber. Their effect is negligible in the NiAl(110) case due to its nonreactive character and the low surface temperature used in the experiments,[8] but it is more important for Pd(111). Since the experimental spectra are reported in arbitrary units, they have been normalized to the theory as indicated in each figure. In addition, the calculated diffraction peaks have been convoluted with a Gaussian function of width σ to account for the limited angular resolution of the detector.

We will begin our discussion with the $D_2/NiAl(110)$ case. The first two spectra (a and b), measured by Farías *et al.*,[29] show in-plane diffraction, which, apart from specular reflection, is the dominant process for this activated system. The third spectrum (c) (Ref. 58) also shows out-of-plane diffraction. It can be seen that all diffraction peaks are more or less reproduced by the classical calculations, including their relative intensities. This is not the case for the specular peak that is underestimated by 54%, 40%, and 24% for the cases shown in panels (a), (b), and (c), respectively. This agreement is worse than in Fig. 3, most likely because the

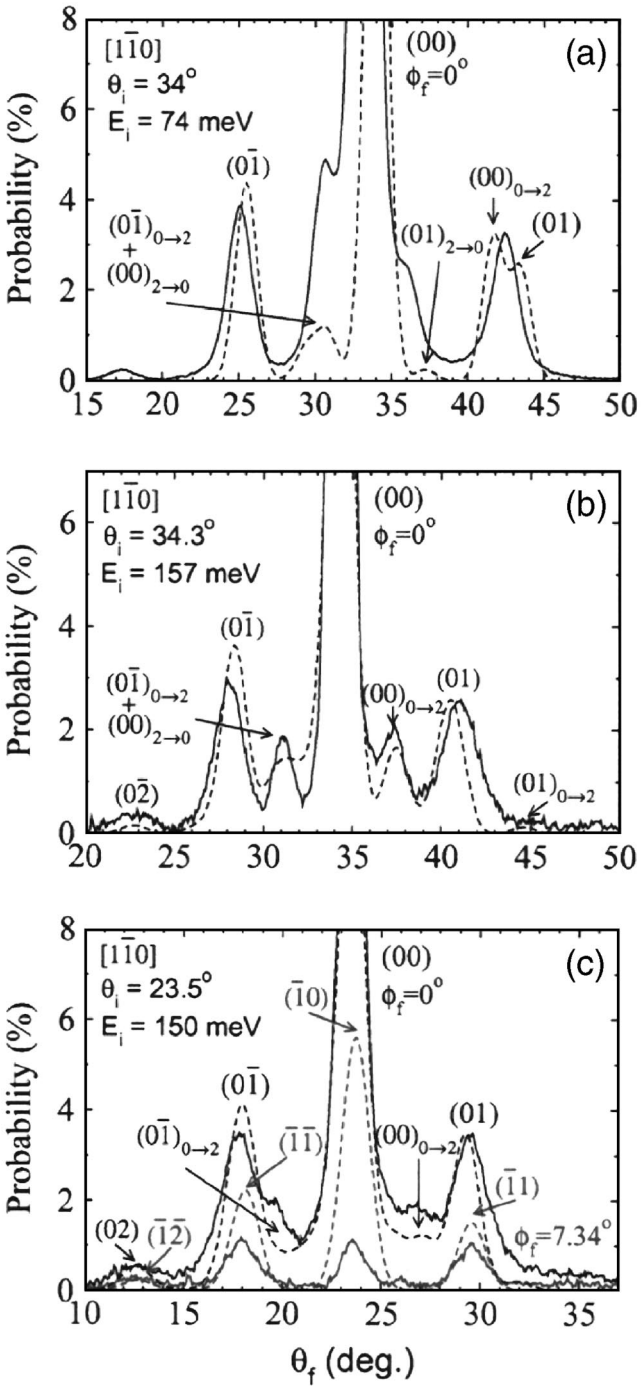

FIG. 4. (Color online) Diffraction spectra for $D_2/NiAl(110)$ at different incidence conditions. Black curves: in-plane diffraction. Green curves: out-of-plane diffraction. Full lines: experimental results (two upper panels, Ref. 29; lower panel, Ref. 58). Dashed lines: results of the classical diffraction method. Theoretical peaks have been convoluted with a Gaussian function of width $\sigma=0.7°$ to account for the limited angular resolution of the experiment. Experimental results have been normalized to the intensity of the largest first-order rotationally elastic diffraction peak with $\theta_f > \theta_i$. Numbers within brackets indicate the incidence plane. ϕ_f is the reflection angle referred to the incidence plane and is related to θ_f and φ_f (see Fig. 1) by the equation: $\sin\phi_f = \sin\theta_f \sin\varphi_f$ (for each experimental spectrum, ϕ_f remains constant). RID peaks are denoted by their Miller indices (n,m) and the rotational transition $J_i \rightarrow J_f$.

incidence energies are smaller, especially for the first case shown in the figure (74 meV). At an incidence energy of 74 meV, the diffraction peak appearing at 42° is the super-

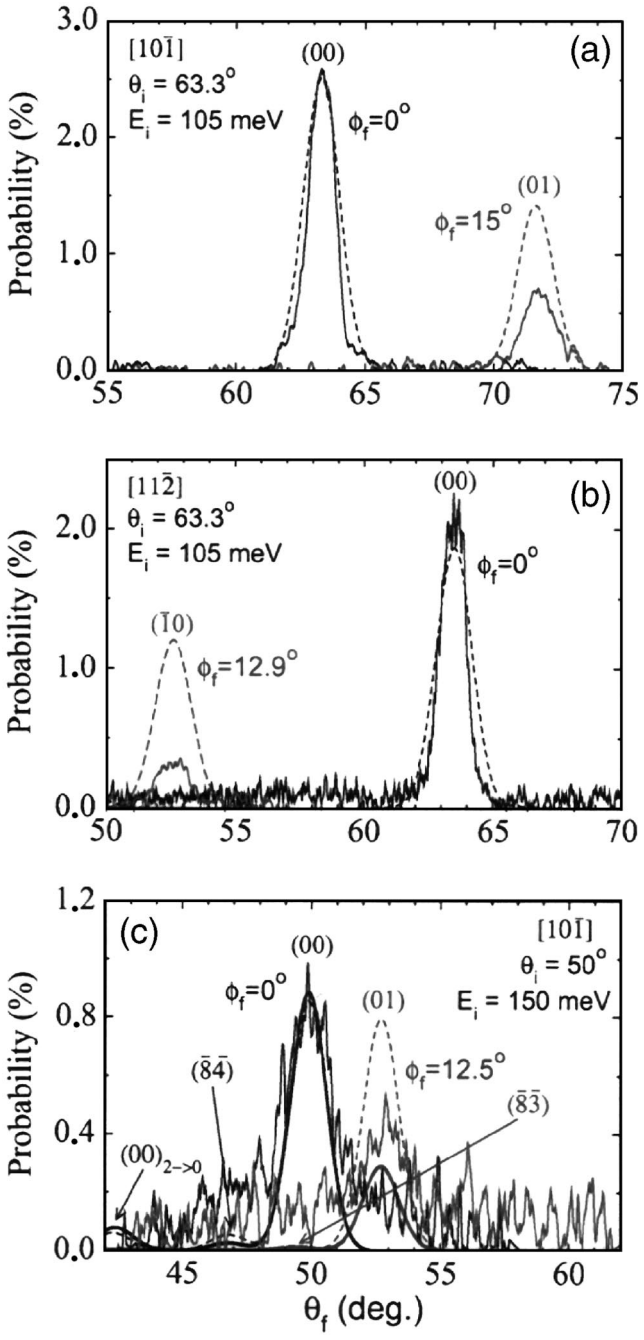

FIG. 5. (Color online) Diffraction spectra for H_2/Pd(111) at different incidence conditions. Black curves: in-plane diffraction. Green curves: out-of-plane diffraction. Full lines: experimental results (two upper panels, Ref. 31; lower panel, Ref. 58). Dashed lines: results of the classical diffraction method. Thick full lines: results of the quantum calculations. Theoretical peaks have been convoluted with a Gaussian function of width σ=0.7° to account for the limited angular resolution of the experiment. Experimental and classical results have been normalized to the intensity of the specular peak obtained in the quantum calculations. Numbers within brackets indicate the incidence plane. The angle ϕ_f is defined as in Fig. 4.

position of the first-order elastic diffraction peak (01) and the $J=0\rightarrow 2$ RID peak $(00)_{0\rightarrow 2}$. This peak was assigned in Ref. 29 as (01). Similarly, the present results allow one to interpret the origin of the two shoulders superimposed on the dominant specular peak: $(01)_{2\rightarrow 0}$ for the structure on the right of the specular peak and $(0\bar{1})_{0\rightarrow 2}+(00)_{2\rightarrow 0}$ for the structure on the left. At higher impact energies [see panel (b)], the same structures are visible, but now elastic peaks are well separated from inelastic peaks. Figure 4(c) shows that classical calculations predict the existence of both in-plane and out-of-plane peaks. The latter are mainly due to elastic diffraction along the $(\bar{1},\bar{1})$, $(\bar{1},0)$, and $(\bar{1},1)$ directions, in good agreement with the measurements. These peaks, however, are overestimated by the classical theory, especially for the $(\bar{1}0)$ transition. It is worth noticing that peaks allowed by Bragg's law but *not* observed in the experiment are not obtained in the classical calculations either. For instance, in the last spectrum shown in Fig. 4, the number of allowed in-plane peaks is 77 (11 elastic and 66 inelastic), while only six of them are observed in the experiment. The situation is similar for out-of-plane diffraction.

We move now to the H_2/Pd(111) system. As mentioned in the Introduction, this is a reactive system and, therefore, diffraction intensities are roughly one order of magnitude smaller than in D_2/NiAl(110). A particularly interesting feature of H_2/Pd(111) concerns the recent observation that, for large incidence angles, most diffraction appears out-of-plane.[31] This is apparent from Figs. 5(a) and 5(b), which show spectra recently measured at an impact energy of 105 meV.[31,61] The dominant out-of-plane diffraction at large incidence angles can be explained on the basis of arguments that are specific to grazing incidence[31,56] and bears no relation to the details of the PES. Interestingly, very recent experiments[58] show that out-of-plane diffraction can also be dominant for more general incidence conditions [i.e., non-grazing incidence, Fig. 5(c)]. In agreement with experiment, classical calculations predict the existence of a single dominant out-of-plane diffraction peak: the (01) peak for incidence along the $[10\bar{1}]$ direction and the $(\bar{1}0)$ one for incidence along the $[11\bar{2}]$ direction. As in the D_2/NiAl(110) case, out-of-plane peaks are overestimated by the classical calculations. This is not the case for quantum calculations. Figure 5(c) shows a comparison between the present results, obtained from both classical and quantum calculations, and experimental data obtained at 150 meV.[58] The agreement between quantum results and the experimental spectra is excellent. This suggests that the PES used for the present calculations is adequate for describing diffraction at collision energies close to 100–150 meV. Thus, the discrepancy between the experimental and the classical intensities for the out-of-plane peak can only be attributed to limitations of classical mechanics. However, it is important to stress again that for all other peaks not seen in the experiments, classical calculations predict a very low intensity in excellent agreement with quantum calculations. For example, among the 33 peaks (5 elastic and 28 inelastic) that are allowed in plane for E_i=150 and θ_i=50°, only the specular one is clearly seen in the experiment and the theory. Classical and quantum calculations shown in Fig. 5 predict the existence of the low intensity peaks $(\bar{8},\bar{3})$ and $(\bar{8},\bar{4})$, but these peaks are not observed due to experimental noise.

VI. CONCLUSIONS

We have presented a 6D classical method to describe diffraction of diatomic molecules from metal surfaces using

ab initio potential energy surfaces. The method consists in discretizing the variation of the parallel linear momentum by defining 2D Wigner–Seitz cells around each lattice point in reciprocal space. We have applied this procedure to investigate diffraction in the nonreactive $D_2/NiAl(110)$ and reactive $H_2/Pd(111)$ systems. Comparisons with experimental results and 6D quantum dynamical calculations for impact energies between 70 meV and 150 meV show that, apart from the dominant specular peak, the method is able to predict the relative intensity of the most important in-plane peaks, as well as which out-of-plane peaks have large intensity. At 200 meV, the agreement between classical and quantum calculations is good even for the specular peak. The absence of many peaks allowed by Bragg's law but not seen in the spectra is exclusively due to the molecule-surface dynamics, which is reasonably described by classical mechanics. Although the present method cannot compete in accuracy with fully quantum mechanical calculations, it has the advantage that it is computationally much cheaper. Thus, it can be used to make reliable predictions about which diffraction peaks should make an important contribution to the diffraction spectrum in those cases where the 6D potential energy surface is known accurately. This can be very helpful to guide experimentalists and to interpret the results of their measurements almost instantaneously.

The most significant advantage of the present method compared with other methods is that it takes into account the full dimensionality of the problem and makes use of realistic PESs obtained from *ab initio* calculations. This is in contrast with current applications of, e.g., the eikonal approach,[26] which require a particular form of the PES (such as the phenomenological hard corrugated wall) and are carried out in 3D to avoid the complexity introduced by the internal molecular degrees of freedom. Finally, the reasonable agreement between classical diffraction intensities and those obtained from quantum calculations or the experiment indicate that the molecule-surface dynamics leading to diffraction is to a large extent classical in nature.

ACKNOWLEDGMENTS

This work was partially supported by the DGI (Spain) under Project Nos. BFM2003-00194 and BQU2001-0147, the Subdirección General de Cooperación Internacional (Spain), the Comunidad de Madrid (Contract No. 07N/0041/2002), and the "Programa Ramón y Cajal" (MCyT). C.D. acknowledges a FPU fellowship of the MECD (Spain) and a Marie-Curie Training Site Fellowship of the European Union. M.F.S. was supported by a CW program grant. The authors thank the Centro de Computación Científica (CCC-UAM, Spain) and the Dutch National Computing Facilities Foundation (NCF) for their generous allocation of computer time. The Surface Science Lab (UAM) gratefully acknowledges K. H. Rieder for the donation of the diffraction apparatus used in the experiments.

[1] *Dynamics of Gas-Surface Interactions*, edited by C. T. Rettner and M. N. R. Ashfold (Royal Society of Chemistry, London, 1991).
[2] G. R. Darling and S. Holloway, Rep. Prog. Phys. **58**, 1595 (1995).
[3] A. Gross, Surf. Sci. Rep. **32**, 291 (1998).
[4] G. J. Kroes, Prog. Surf. Sci. **60**, 1 (1999).
[5] K. Christmann, *Introduction to Surface Physical Chemistry* (Springer, New York, 1991).
[6] M. F. Bertino and J. P. Toennies, J. Chem. Phys. **110**, 9186 (1999).
[7] A. C. Luntz, J. K. Brown, and M. D. Williams, J. Chem. Phys. **93**, 5240 (1990).
[8] M. F. Bertino, F. Hofmann, and J. P. Toennies, J. Chem. Phys. **106**, 4327 (1997).
[9] D. Rendulic, G. Anger, and A. Winkler, Surf. Sci. **208**, 404 (1989).
[10] C. T. Rettner, D. J. Auerbach, and H. A. Michelsen, Phys. Rev. Lett. **68**, 1164 (1992).
[11] C. T. Rettner, Phys. Rev. Lett. **69**, 383 (1992).
[12] H. A. Michelsen, C. T. Rettner, and D. J. Auerbach, Phys. Rev. Lett. **69**, 2678 (1992).
[13] H. Hou, S. J. Gulding, C. T. Rettner, A. M. Wodtke, and D. J. Auerbach, Science **277**, 80 (1997).
[14] T. Mitsui, M. K. Rose, E. Fomin, D. F. Ogletree, and M. Salmeron, Nature (London) **422**, 705 (2003).
[15] T. Mitsui, M. K. Rose, E. Fomin, D. F. Ogletree, and M. Salmeron, Surf. Sci. **540**, 5 (2003).
[16] A. Hodgson, J. Moryl, P. Traversaro, and H. Zhao, Nature (London) **356**, 501 (1992).
[17] C. T. Rettner, D. J. Auerbach, and H. A. Michelsen, Phys. Rev. Lett. **68**, 2547 (1992).
[18] M. Gostein, H. Parhikhteh, and G. O. Sitz, Phys. Rev. Lett. **75**, 342 (1995).
[19] A. Hodgson, P. Samson, A. Wight, and C. Cottrell, Phys. Rev. Lett. **78**, 963 (1997).
[20] M. Gostein and G. O. Sitz, J. Chem. Phys. **106**, 7378 (1997).
[21] M. Gostein, E. Watts, and G. O. Sitz, Phys. Rev. Lett. **79**, 2891 (1997).
[22] E. Watts and G. O. Sitz, J. Chem. Phys. **111**, 9791 (1999).
[23] E. Watts, G. O. Sitz, D. A. McCormack *et al.*, J. Chem. Phys. **114**, 495 (2001).
[24] G. R. Darling and S. Holloway, J. Chem. Phys. **97**, 734 (1992).
[25] A. Cruz and B. Jackson, J. Chem. Phys. **94**, 5715 (1991).
[26] D. Farías and K. H. Rieder, Rep. Prog. Phys. **61**, 1575 (1998).
[27] M. F. Bertino, A. P. Graham, L. Y. Rusin, and J. P. Toennies, J. Chem. Phys. **109**, 8036 (1998).
[28] C.-F. Yu, K. B. Whaley, C. S. Hogg, and S. J. Sibener, J. Chem. Phys. **83**, 4217 (1985).
[29] D. Farías, R. Miranda, and K. H. Rieder, J. Chem. Phys. **117**, 2255 (2002).
[30] D. Cvetko, A. Morgante, A. Santaniello, and F. Tommasini, J. Chem. Phys. **104**, 7778 (1996).
[31] D. Farías, C. Díaz, P. Nieto, A. Salin, and F. Martín, Chem. Phys. Lett. **390**, 250 (2004).
[32] M. Bertino and D. Farías, J. Phys.: Condens. Matter **14**, 6037 (2002).
[33] J. D. Doll, J. Chem. Phys. **59**, 1038 (1973).
[34] J. D. Doll, J. Chem. Phys. **61**, 954 (1974).
[35] J. H. McCreery and G. Wolken, J. Chem. Phys. **63**, 4072 (1975).
[36] J. H. McCreery and G. Wolken, Chem. Phys. Lett. **39**, 478 (1976).
[37] C. Díaz, H. F. Busnengo, F. Martín, and A. Salin, J. Chem. Phys. **118**, 2886 (2003).
[38] H. F. Busnengo, W. Dong, P. Sautet, and A. Salin, Phys. Rev. Lett. **87**, 127601 (2001).
[39] A. D. Kinnersley, G. R. Darling, S. Holloway, and B. Hammer, Surf. Sci. **364**, 219 (1996).
[40] H. F. Busnengo, E. Pijper, G. J. Kroes, and A. Salin, J. Chem. Phys. **119**, 12553 (2003).
[41] E. Pijper, M. F. Somers, G. J. Kroes, R. A. Olsen, E. J. Baerends, H. F. Busnengo, A. Salin, and D. Lemoine, Chem. Phys. Lett. **347**, 277 (2001).
[42] D. G. Truhlar and J. T. Muckerman, in *Atom-Molecule Collision Theory: A Guide for the Experimentalist*, edited by R. B. Berstein (Plenum, New York, 1979), p. 505.
[43] L. Bonnet and J. C. Rayez, Chem. Phys. Lett. **397**, 106 (2004).
[44] C. J. Ray and J. M. Bowman, J. Chem. Phys. **63**, 5231 (1975).
[45] C. J. Ray and J. M. Bowman, J. Chem. Phys. **66**, 1122 (1977).
[46] S. C. Park and J. M. Bowman, Chem. Phys. Lett. **110**, 383 (1984).
[47] S. Saini, D. A. Dows, and H. S. Taylor, Chem. Phys. **90**, 87 (1984).
[48] R. B. Gerber, Chem. Rev. (Washington, D.C.) **87**, 29 (1987).
[49] H. F. Busnengo, C. Crespos, W. Dong, J. C. Rayez, and A. Salin, J. Chem. Phys. **116**, 9005 (2002).
[50] P. Rivière, H. F. Busnengo, and F. Martín, J. Chem. Phys. **121**, 751 (2004).

[51]J. P. Perdew, Phys. Rev. B **33**, 8822 (1986).
[52]A. D. Becke, Phys. Rev. A **38**, 3098 (1988).
[53]C. Crespos, H. F. Busnengo, W. Dong, and A. Salin, J. Chem. Phys. **114**, 10954 (2000).
[54]H. F. Busnengo, A. Salin, and W. Dong, J. Chem. Phys. **112**, 7641 (2000).
[55]R. A. Olsen, H. F. Busnengo, A. Salin, M. F. Somers, G. J. Kroes, and E. J. Baerends, J. Chem. Phys. **116**, 3841 (2002).
[56]E. Pijper, G. J. Kroes, R. A. Olsen, and E. J. Baerends, J. Chem. Phys. **117**, 5885 (2002).
[57]J. K. Vincent, R. A. Olsen, G. J. Kroes, M. Luppi, and E. J. Baerends, J. Chem. Phys. **122**, 044701 (2005).
[58]D. Farías, C. Díaz, P. Rivière *et al.*, Phys. Rev. Lett. **93**, 246104 (2004).
[59]J. P. Cowin, C.-F. Yu, S. J. Sibener, and J. E. Hurst, J. Chem. Phys. **75**, 1033 (1981).
[60]T. Engel and K. H. Rieder, Surf. Sci. **109**, 140 (1981).
[61]C. Díaz, H. F. Busnengo, P. Rivière, F. Martín, A. Salin, P. Nieto, and D. Farías, Phys. Scr., T **110**, 394 (2004).